

A Conceptual Design and Optimization Method for Blended-Wing-Body Aircraft

Roelof Vos* and Jorrit van Dommelen†

Delft University of Technology, Delft, The Netherlands

This paper details a new software tool to aid in the conceptual design of blended-wing-body aircraft. The tool consists of four main modules. In the preliminary sizing model a class I estimate of the maximum take-off weight, wing loading, and thrust-to-weight ratio is calculated. This information is used together with an initial guess of the 30 design variables that to form a geometric model of the aircraft. From this geometric model four disciplinary models are derived: an aerodynamic model, a model of the wing box structure, a model for the cabin, and a model for the fuel tank. In the subsequent analysis module refined weight estimation for the operating-empty weight is being calculated, as well as the center-of-gravity shift during loading, the static margin, the main stability and control derivatives, and the harmonic range. In the last module, these analysis results are compared to 27 nonlinear constraints stemming from the top-level requirements and the aviation regulations. A gradient-based optimization routine is employed to find a combination of the design variables that satisfies all constraints while optimizing for harmonic range at constant maximum take-off weight. Between 20 and 60 iterations are required to achieve convergence. The tool has been set-up to allow for maximum configurational flexibility such as forward-swept outer wings, under-the-wing engines, and twin vertical tails.

I. Introduction

For conventional aircraft configurations, such as the tube-and-wing (TAW) aircraft, commercially-off-the-shelf (COTS) design tools are available for their conceptual design. Traditionally, these tools are based on proven handbook methods and embedded in a software package (e.g. DARcorp's AAA or PASS by Desktop Aeronautics). Typically, these packages reduce top-level requirements along with constraints on handling qualities and safety to a Class II airplane design. Subsequently, the design is further refined at the preliminary design level where the fidelity of the analysis tools increases progressively.

At TU Delft continuous efforts have been directed towards the implementation of a design and engineering engine (DEE) that can facilitate multi-disciplinary design optimization (MDO) beyond the Class II. One important benefit is the ability of the DEE to analyze and size both conventional and unconventional configurations. As was demonstrated by Schut *et al.*, the initial input vector for the DEE plays a pivotal role in whether all the constraints can be met once the MDO process has converged.¹ It was argued that a separate lower-fidelity DEE would be necessary to define an input vector that would yield feasible solutions in the subsequent optimization process. This lower-fidelity DEE was termed the conceptual DEE because it translated the top-level requirements to an initial input vector for the subsequent MDO process. Likewise, the output from the subsequent DEE could be used as an input vector for a more advanced DEE, enabling a multi-fidelity design and optimization process. This process is schematically depicted in Figure 1.

Considering the case of TAW aircraft, the very first initiator DEE is readily available in the form of the aforementioned Class II airplane design tools. Because these tools are based on empirical relationships, the likelihood of having a feasible design as an output of this first design step is rather high. For non-traditional aircraft configurations, there are no recipes that ensure a feasible design at the end of the conceptual design phase. On the other hand, it is desirable to assess different configurations on their feasibility at

*Assistant Professor, Faculty of Aerospace Engineering at Delft University of Technology, Kluyverweg 1, 2629 HS Delft, The Netherlands, AIAA member

†Engineer at Barge Master, Karel Doormanweg 9, 3115 JD Schiedam, The Netherlands

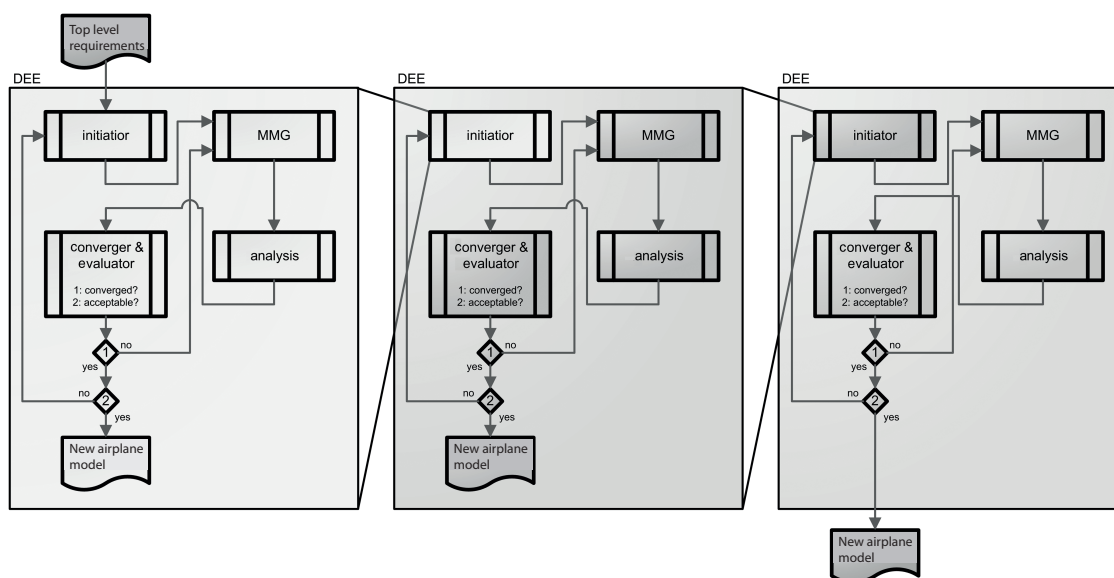


Figure 1. Initiator Component of a DEE Consists of Multiple DEEs of Simplified Problems (Modified from Schut *et al.*¹)

low computational cost. The internal optimization loop within the first DEE ensures that for a given configuration, a limited number of design variables, and a reduced set of constraints, a design results that has a high probability of being feasible. With carefully chosen sizing methods, analysis tools, and optimization algorithms this can swiftly result in an adequate input vector for the subsequent DEE.

Of all the non-traditional airplane designs, the blended wing body is one of the few concepts that is currently considered by academia and industry as a possible successor to the TAW aircraft. The idea of having the body generate part of the lifting forces, thereby reducing the overall wetted area of the airplane dates back to the early 20th century when airplane designers such as Dunne, Lippisch, and the Horton brothers invented several all-lifting-vehicle (ALV) configurations.² Prior to World-War II Northrop developed the X-35 flying wing (FW). After the war the X-35s were retrofitted with turbojet engines to become the B-49 bomber. Even though speed and altitude performance of the B-49 were good, the airplane lacked sufficient range and was canceled in favor of the Convair B-36. It was speculated that the range inferiority was inherent to the jet-powered FW configuration.³ Due to this controversy, the flying-wing concept was abandoned for almost 40 years. It revived in the early 1990s with the introduction of the Northrop B-2, demonstrating the feasibility of a high-speed FW aircraft. It also resulted in renewed discussion about the aerodynamic performance of FW aircraft compared to TAW aircraft. An independent examination by Torvik on the range performance of high-bypass-ratio FW aircraft demonstrated that prior assumptions on aspect ratio and wing thickness substantiating the conclusion that FW aircraft had inferior range performance were not correct.⁴

In 1991 a paper by Torenbeek compared aircraft of various wing volume to total volume ratios (X). He recognized that the low wing loading of an FW aircraft results in a reduced aerodynamic efficiency at FL350. A higher lift-to-drag ratio can only be achieved if the airplane is flown at higher altitude. Because engine thrust is linearly dependent on the ambient pressure in the stratosphere, the size of the engine is likely to grow with a higher cruise altitude. Torenbeek confirms this and comes to the following conclusions based on a simplified analysis:⁵

- The highest aerodynamic efficiency for a baseline TAW aircraft with $X = 0.18$ occurs for $T/p = 9\text{m}^2$ and amounts to $L/D = 20.5$.
- For engines with an installed thrust of $T/p = 9\text{m}^2$ the FW aircraft ($X = 0.9$) does not perform better than the TAW aircraft, while L/D decreases rapidly with decreased installed thrust.
- To reach its full potential, the FW aircraft requires 45% more thrust to reach the maximum $L/D = 27.5$.
- To achieve this L/D , the FW aircraft needs to cruise at FL450.

These conclusions were based on a hypothetical airliner with a gross weight of 450 tons, a cruise Mach number of 0.85 and a total useful volume of 2000m³. Furthermore, it was assumed that the drag polar

could be represented by a simple two-term quadratic equation. These results indicated that the FW aircraft certainly had the potential to improve the aerodynamic efficiency of a new generation of aircraft, provided that they would fly at higher altitudes.

In 1951 it was Burnelli who conceived a design that bears close resemblance to what is commonly known as the blended wing body (BWB) aircraft (see Figure 2). Since the 1980s Russian studies at TsAGI have investigated the BWB concept and the technologies that are required to making them viable.⁶ Developments at McDonnell Douglas (later Boeing) throughout the 1990s confirmed the findings by Torvik and Torenbeek by predicting a 20% higher lift-to-drag ratio for an 800 passenger BWB airplane compared to a conventional baseline aircraft with equal capacity and range.⁷ Subsequent research by Boeing and NASA on the BWB-450 demonstrated to have 32% better fuel burn properties compared to the Airbus A380, using similar technology levels.⁸ Test flights to investigate the performance and handling qualities on scale model (X48-B) have been under way since 2007, with overall satisfactory results. Flight tests of a modified BWB configuration with twin vertical tails (X-48C) to shield engine noise were scheduled to take place in late 2011.⁹



Figure 2. Photograph of a Model Of Burnelli's Advanced Transport Design from 1951¹⁰

Multi-disciplinary optimization (MDO) has been demonstrated to be of great help in improving baseline BWB designs. Due to the tight interconnection between wing planform shape and cabin volume allocation, the optimization is significantly more complicated than for a traditional TAW aircraft. Given the short-coupled nature of the aircraft in combination with the absence of an empennage complicates the problem even more by making the planform shape responsible for the aerodynamic performance, balance, stability, and control of the airplane. To refine the design of the BWB-450 a multi-disciplinary design tool (WingMOD) was used to size the aircraft for performance, balance, stability, and control.^{11,12} Starting point for the optimization was an aft-swept configuration with winglets doubling as vertical tails. In Europe a collaborative project on the multi-disciplinary optimization of the BWB relied on distributed analysis tools that were connected to a single MMG.¹³ Both projects demonstrated how the total weight of the BWB airplane could successfully be reduced while satisfying all the constraints stemming from regulations and top-level requirements.

To facilitate MDO a parametric description of the airplane geometry based on high-level primitives (HLPs) can swiftly generate geometric models of many diverse aircraft configurations.¹⁴ Combining and resizing the HLPs allows the designer to generate airplane designs beyond the TAW, such as the BWB configuration¹³ (see Figure 3). The design can be subjected to various analysis tools (aerodynamic,¹⁵ structural,¹⁶ aeroelastic,¹⁷ acoustic¹⁸) each based on a single representation of the geometry. The results of these modules can subsequently be used in flight mechanics tools to investigate performance and handling qualities.^{19,20} The interface between the analysis tools and the geometry module is formed by so-called capability modules (CMs) that translate the geometry to tool-specific input files. The output from each of the analysis tools can be used in an optimization process by comparing it to the constraints and evaluating the objective function. The assembly of the HLP-based geometry module and the various CMs has been termed the multi-model generator (MMG). Together with the analysis tools, the optimization module, and the initial input vector it forms the design and engineering engine (DEE).

Even though it has been demonstrated that MDO can successfully be used to improve existing BWB designs in various ways, implementation in the conceptual design has been limited to aerodynamic and structural analysis.²¹ At the same time, no conceptual design tools are available to quickly size various BWB configurations. Finally, if the multi-fidelity design optimization paradigm of Figure 1 is to be successfully implemented altering the BWB configuration should be enabled whenever a configuration proves to be infeasible in any of the lower level DEEs. This paper details a first step in the generation of the initial DEE

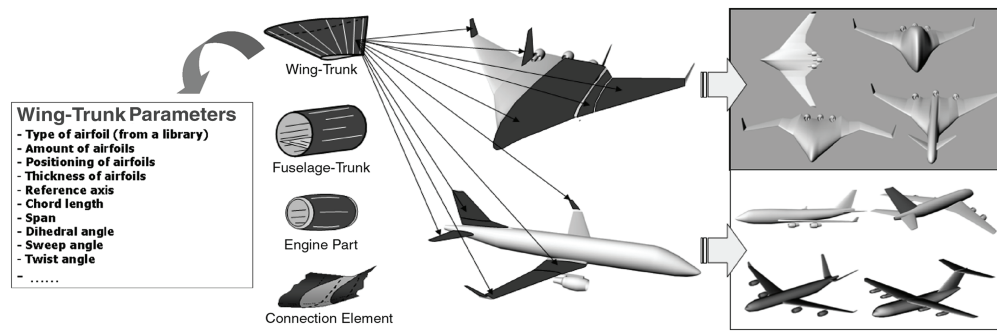


Figure 3. The High-Level Primitives Build Up Approach¹⁴

that allows for various BWB configurations to be analyzed with relatively low-fidelity tools, resulting in a Class II design of the BWB. Engine positioning, fin positioning, wing sweep, and landing gear disposition are included in the configuration design. The following sections detail the methods that have been implemented in the tool and discuss some of the obtained results.

II. Methodology

A. Conceptual DEE Structure

The conceptual DEE consists of four modules (see Fig. 4). The initiator module generates an input vector based on traditional preliminary sizing methods. Subsequently, the MMG constructs a geometric model of the aircraft and generates a simple aerodynamic and structural model. It also sizes fuel tank and cabin. In the analysis module, the aerodynamic forces are evaluated, the weight and center-of-gravity (CoG) travel are calculated, and the airplane is trimmed. Stability and control derivatives are calculated, the rotation speed, the minimum control speed, and the cruise range are determined. In the evaluator module the analysis results are compared to set constraints. The optimization routine tries to satisfy all the constraints and subsequently find the airplane geometry with the longest range. Whenever the constraints are not met (“acceptable?”) or the optimization has not converged (“converged?”), the optimizer alters the input vector and runs the loop again.

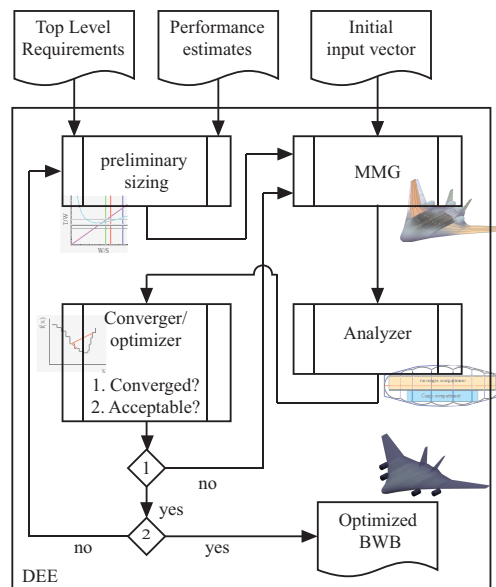


Figure 4. Structure of DEE for Conceptual Design of the BWB

B. Preliminary Sizing

During preliminary sizing the top-level requirements along with the relevant certification specifications are used to estimate the maximum take-off weight, thrust and wing surface area. The wing loading and thrust loading are sized in the initiator based on requirements on range, take-off field length, cruise speed, and cruise altitude. Assumptions on maximum lift coefficients in the relevant configurations as well as statistical data on characteristic weights are made based on values from literature on BWB aircraft. In Fig. 5 the outline of the preliminary sizing module is shown. The output of the preliminary sizing along with configurational choices on the number of and position of engines, the fin position, and the wing sweep (forward or aft) are input to the subsequent module (MMG).

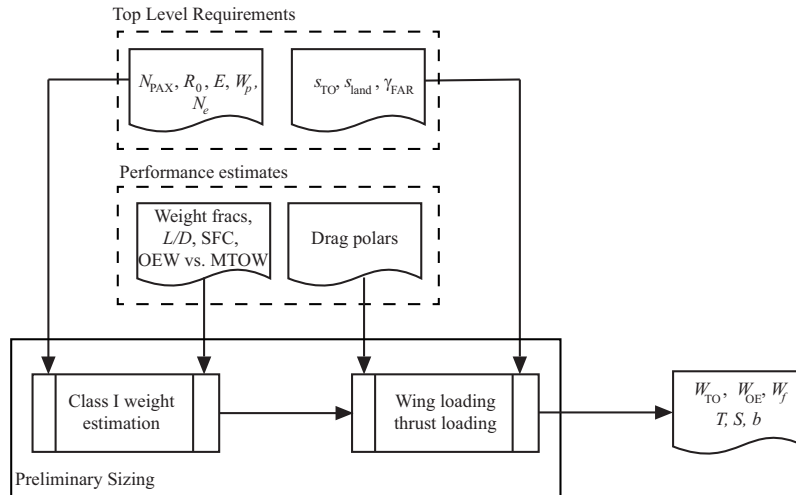


Figure 5. Structure of Preliminary Sizing Module

C. Multi-Model Generator

The MMG receives input from the preliminary sizing module and the vector containing the initial design parameters. This input vector is automatically scaled such that the wing span and wing area match those calculated in the preliminary sizing. The MMG translates this information into a geometric model of the outer shell of the aircraft. The BWB planform is translated into five individual wing trunks. Each trunk has a root and tip airfoil that needs to be selected by the user. In addition, initial values for sweep, taper, span, twist, relative thickness, and mean chord are set by default in the input vector. During the optimization, these parameters are changed. For the vertical tail a single input parameter can be selected (tail height). All other geometric parameters of the vertical tail have either been fixed or related to the tail height via a fixed relation. This has been done to keep the number of design variables as low as possible. In total there are 30 design variables (excluding airfoil shapes for each of the sections). An example of an input vector for the planform shape is presented in Table 1.

Parameter	Sect 1	Trunk 1	Sect 2	Trunk 2	Sect 3	Trunk 3	Sect 4	Trunk 4	Sect 5	Trunk 5	Sect 6	Unit
Chord	38.5		37.9		33.2		22.5		12.7		4.2	m
Span		1.0		2.7		5.7		8.9		21.4		m
Twist									1.0		1.0	deg
Sweep		31		63		55		44		38		deg
Dihedral		0		0		1.0		2.0		5.0		deg
Thickness-to-chord ratio	0.16		0.16		0.16		0.16		0.12		0.12	-

Table 1. Example Input Vector for BWB Planform.

A particular configuration is specified by the input data, which consists of four input variables. The input variables consist of the vertical tail type, the engine vector prescribing the location of each engine, the airfoil vector, describing the airfoils used at each section and finally the input vector, which is used in the optimization. An example of the input data used is given in Table 2. In this example the airplane configuration has four engines, which are all positioned on top of the body at a predefined distance from the trailing edge. The airfoil shapes are also defined at each of the sections, although it should be noted that the thickness-to-chord ratio is automatically scaled by the input vector of Table 1.

Variable	Input
Vertical tail type	'winglet'
Engine vector	'body' 'body' 'body' 'body'
Airfoil vector	'NACA0017' 'NACA0017' 'NACA0016' 'NACA0014' 'SC(2)0012' 'SC(2)0010'

Table 2. Example Input for BWB Configuration.

Based on the initial input vector and the geometric values calculated during the Preliminary Sizing a geometric model of the BWB is constructed. A continuous surface is lofted between the root and tip airfoils of each of the airfoils. From this geometric model the MMG generates three disciplinary models First, a geometric model for the torque box, the fuel tank, and the cabin are constructed. In addition, a panel distribution of the planform is generated to be used by a vortex-lattice method (VLM). A schematic overview of the entire MMG module is presented in Fig. 6.

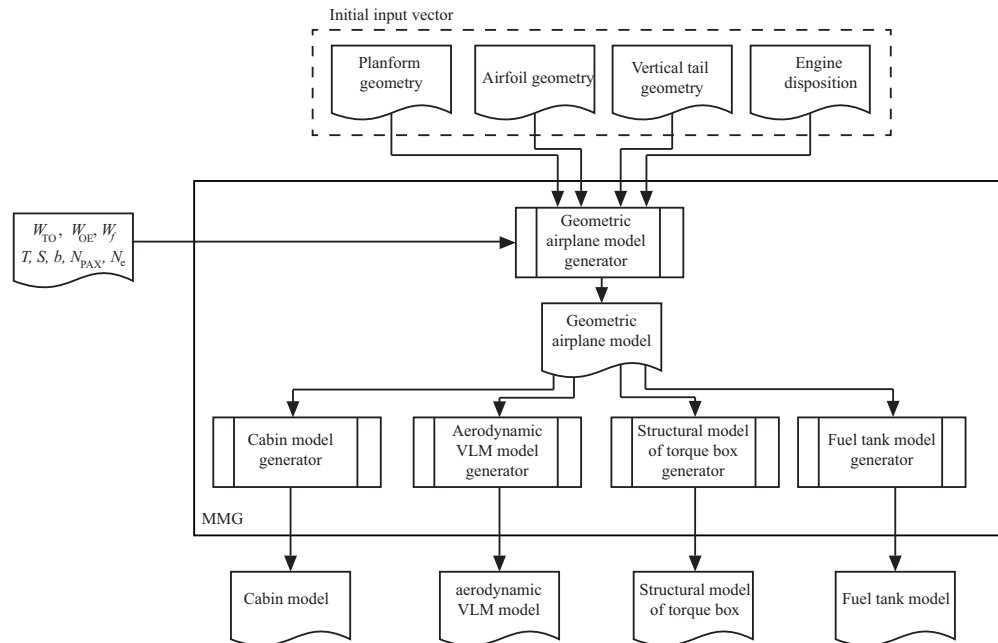


Figure 6. Structure of Multi-Model Generator

An important assumption that has been made in the construction of the pressure cabin is that it consists of a multi-bubble interior to carry the pressure loads. An aerodynamic shell encloses the multi-bubble cabin. Multi-bubble supremacy over stiffened panels was demonstrated for passenger aircraft by Mukhopadhyay *et al.*²² and was therefore selected in this module. The multi-bubble cabin automatically scales according to the geometry of the aerodynamic shell around it. The main deck floor is automatically constructed, along with a cargo floor, whenever there is sufficient space to store a minimum of one LD3-45 container. The fuel tank and torque box are also dimensioned based on the outer geometry of the wing and body trunks. An overview of these components is shown in Fig. 7.

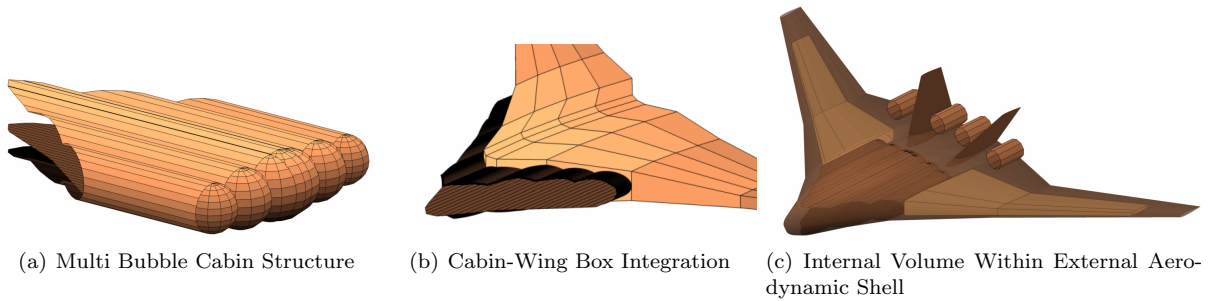


Figure 7. Example of Internal and External Geometric Models

D. Analysis Modules

In Fig. 8 the analysis modules are shown. In the cabin analysis the cabin volume, main deck surface area, and cargo volume are calculated. This is based on the geometric input from the MMG. The aerodynamic analysis consists of a vortex lattice solver (Tornado²³) that provides all aerodynamic coefficients (including an estimation of the friction drag based on strip theory) and also the lift distribution. In addition, control derivatives are calculated for the rudder(s) and elevator(s). Finally, the spanwise location of the highest loaded section is located. Based on the maximum lift coefficient of this section ($c_{l_{max}}$ is a function of the local airfoil shape) and the associated lift distribution the maximum lift coefficient of the wing ($C_{L_{max}}$) is calculated along with the stall angle-of-attack.

A Class II component weight estimation is based on traditional handbook methods^{24, 25} where wing weight is estimated based on Torenbeek's approach.²⁶ Furthermore, a weight estimation for the unorthodox cabin was developed by Geuskens *et al.*²⁷ and has been implemented in the Class II weight estimation. Subsequently, the center of gravity (CoG) of each of the components is determined resulting in the airframe CoG. Various loading and unloading strategies for both passengers and fuel are investigated to determine the operational implementation that results in the minimum CoG travel. This scenario determines the CoG position as a function of the instantaneous airplane weight.

A trim and stability analysis is carried out using the information from the CoG analysis and the aerodynamic analysis. Directional and longitudinal stability derivatives are calculated at most aft position of the CoG. Finally, a performance analysis is performed based on the aerodynamic analysis, the trim drag, the available fuel, and a user-specified value for the specific fuel consumption.

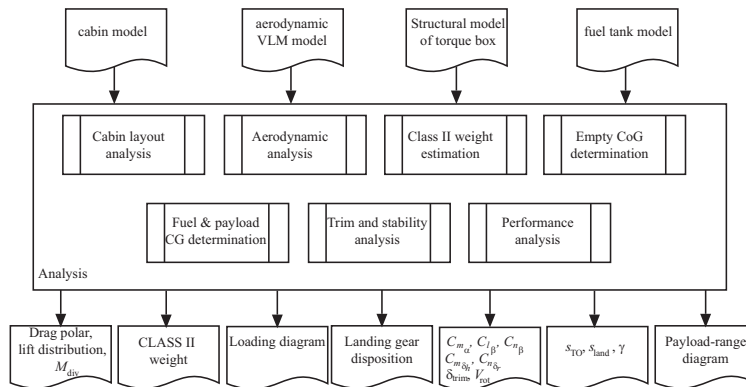


Figure 8. Structure of Analysis Module

The sequence of the analysis models is predetermined. The first analysis tools require only require direct input from the MMG. Subsequent analysis modules rely on the analysis results from the initial models. The feed-forward of analysis results is intuitively depicted by the N₂ chart of Figure 9. It can be seen that in particular the last three analysis tools (i.e. the CoG analysis, stability and control analysis, and performance analysis) rely heavily on the results of the preceding analysis modules.

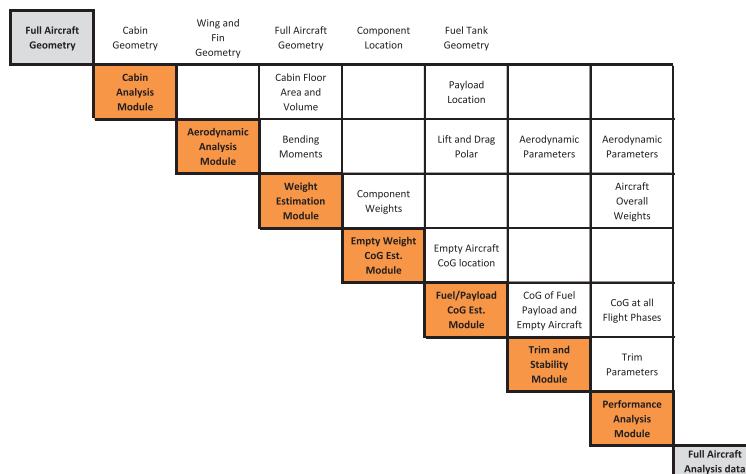


Figure 9. Analysis Module N₂ chart

E. Constraints Analysis and Optimization Procedure

The numerical output from each of the analysis modules is compared to predefined constraints. These include, but are not limited to, constraints on longitudinal and directional stability, rotation speed, minimum control speed with OEI, climb requirements with OEI, trim deflections, cabin volume, and nose wheel loads. Based on the outcome of the constraints analysis the input vector is altered by a predefined increment, dx . To allow for a gradient-based optimization, the increment for each of the design variables is different. In Table 4 an overview of the design variables per wing trunk is shown with their respective values for dx . As can be seen from this table, a total of 30 design variables are present in the optimization procedure. Geometric constraints on leading and trailing edge sweep are incorporated to limit sharp kinks in the planform area (especially the outboard wing) that have been shown to result in large wave drag penalties.⁶

The constraints module collects the calculated data and all constraints implied by aviation authorities, requirements and user supplied constraints. The constraints are placed in a constraints vector, which is used by the optimizer to make optimization decisions. The constraints are summarized in Table 3. Notice that the longitudinal and lateral tip-over constraints are absent from this table. These constraints have already been used to size the length and disposition of the landing gear struts. All of the designs therefore comply with these constraints. Furthermore, it can be observed that the minimum static margin (for the most-aft CoG position) is -10%, which means that the aircraft is allowed to be longitudinally unstable. It has been assumed that with such a static margin it is still possible to realize artificial static stability through fly-by-wire and a dedicated control algorithm.

Beside the constraints calculated in the constraints module, there are four linear constraints applied to the geometry. These linear constraints are necessary to create a workable aircraft geometry. The following linear constraints are implemented:

- Span of a section needs to be larger than the span of the previous section
- Chord has to decrease along the span
- Thickness-to-chord ratio has to decrease along the span
- Leading edge sweep of the two outer most sections must be decreasing

To ensure an equal weight of all the constraints in the optimization process, all of the constraints are normalized with respect to their initial value.

The optimization routine is based on the function `fmincon` in MATLAB. The function `fmincon` is a constrained nonlinear optimization function that finds the minimum of a constrained scalar function of several variables starting with an initial estimate.²⁸ To simplify the optimization procedure it has been chosen to use the harmonic range as the performance parameter to be maximized (i.e. minimize R_0/R). The top-level requirement on range (R_0) that was used in the Class I weight estimation can therefore be

Table 3. Constraints summary

Parameter	Constraints	Unit
Wing span	$b < 80$	m
Aircraft overall length	$l < 80$	m
Cabin floor area	$S_{\text{cabin}} \geq S_{\text{cabin,req}}$	m ²
Cargo volume	$V_{\text{cargo}} \geq V_{\text{cargo,req}}$	m ³
Take-off distance	$s_{\text{TO}} \leq s_{\text{TO,req}}$	m
Landing distance	$s_{\text{land}} \leq s_{\text{land,req}}$	m
Stall speed take-off	$V_{\text{stall,TO}} \leq V_{\text{stall,TO,req}}$	m/s
Stall speed clean	$V_{\text{stall}} \leq V_{\text{stall,req}}$	m/s
Climb gradient OEI1	$\gamma_{\text{OEI1}} > 0.012$	–
Climb gradient OEI2a	$\gamma_{\text{OEI2a}} > 0.000$	–
Climb gradient OEI2b	$\gamma_{\text{OEI2b}} > 0.000$	–
Climb gradient OEI2c	$\gamma_{\text{OEI2c}} > 0.012$	–
Climb gradient OEI3	$\gamma_{\text{OEI3}} > 0.032$	–
Climb gradient AOE1	$\gamma_{\text{AOE1}} > 0.021$	–
Maximum trim deflection	$\delta_h < 12$	deg
Minimum static margin	$\text{SM} > -10$	%
Directional stability	$C_{n_\beta} = 0.010$	–
Dihedral effect	$C_{l_\beta} < 0$	–
Take-off rotation speed	$V_{\text{rot}} < V_{\text{stall,TO}}$	m/s
Drag divergence Mach	$M_{\text{DD}} \leq M_{\text{cruise}}$	–
Nose wheel load	$0.05 < F_{\text{nlg}} < 0.20$	–
Nose landing gear position	$x_{\text{nlg}} > x_{\text{nose}} + 0.5$	m
Main landing gear position	$x_{\text{le}} < x_{\text{mlg}} < x_{\text{te}}$	m

exceeded. Because this is a gradient-based optimization procedure, it is not guaranteed that the local minimum that is found by the optimizer is also the global minimum. The initial input vector for each of the design variables is therefore an important factor in whether a global or a local optimum is found. At the same time this input vector also has a configurational implication. In this sense, the designer can evaluate different BWB configurations by altering the initial input vector. For example, a forward swept configuration (and associated input vector) is likely to result in a different minimum than an aft-swept configuration. This way, the designer can evaluate the result of configurational changes on the range performance of the BWB.

One of the requirements of gradient-based optimization is that the response function is smooth over the entire domain of the design variables. To satisfy this requirement any change in the design variables should be sufficiently large to induce a change in the response function. However, it should not be too large to prevent a wrongfully calculated value for the gradient. It has been investigated what the minimum changes (dx) in the respective design variables should be in order to meet both requirements. The results that have been used in the optimization are displayed in Table 4.

Table 4. dx values per entry

Parameter	Entry	dx	Unit
Chord	$x_1 - x_6$	0.05	m
Span	$x_7 - x_{11}$	0.05	m
Twist	$x_{12} - x_{13}$	0.1	deg
Sweep	$x_{14} - x_{18}$	0.5	deg
Dihedral	$x_{19} - x_{23}$	0.1	deg
Thickness-to-chord ratio	$x_{24} - x_{29}$	0.0025	(-)
Tail Height	x_{30}	0.05	m

Finally, each of the design variables can be varied over a predefined domain. The bounds are chosen such

that they are flexible and will work for BWB with different sizes. The chord and span bounds are the only bounds that are dependent on the size of the aircraft. For example a smaller BWB, designed to carry 200 passengers, will have a smaller wing span. The twist, sweep, dihedral and thickness ratio are independent of the size. The chord and span values are chosen such that smaller and very large BWB are possible without changing the values of the bounds.

Parameter		Sect 1	Trunk 1	Sect 2	Trunk 2	Sect 3	Trunk 3	Sect 4	Trunk 4	Sect 5	Trunk 5	Sect 6	Unit
Chord	\geq	20		20		10		8		4		0.1	m
	\leq	60		60		50		30		20		10	m
Span	\geq		1		2		4		10		20		m
	\leq		5		10		15		30		50		m
Twist	\geq									-3		-5	deg
	\leq									3		5	deg
Sweep	\geq		10		30		20		10		10		deg
	\leq		60		80		80		60		60		deg
Dihedral	\geq		-1		-5		-5		-5		-5		deg
	\leq		1		5		5		5		5		deg
Thickness-to-chord ratio	\geq	0.14		0.14		0.10		0.07		0.06		0.06	-
	\leq	0.19		0.19		0.18		0.18		0.15		0.15	-

Table 5. Lower and upper bounds of input vector for an aft-swept BWB

III. Results and Discussion

The objective of the conceptual DEE is to swiftly design and analyze a BWB configuration relying on simple estimation methods. To demonstrate the result of this design and optimization tool an example configuration is chosen to be optimized. The configuration selected is a configuration with four body mounted engines, a twin vertical tail, mounted on the body and aft-swept wings. The input vector is displayed in Table 1. This vector is the non-scaled input vector and will be scaled by the preliminary sizing to obtain a matching wing area and wing span. Using the input vector, together with the engine vector, vertical tail type and airfoil vector, the optimization is started. A single iteration takes approximately 6 minutes^a and 20 to 60 iterations are required to find a converged solution. The amount of required iterations depends on the start vector and how many iterations it takes to fulfill all constraints. For the current example, 42 iterations were required to find an optimum.

The overall progress of the optimization is displayed in Figure 10. It shows three plots: the function value (R_0/R) at each iteration, the maximum constraint value at each iteration, and the harmonic range at each iteration. After 18 iterations, the aircraft is feasible and the solution starts to converge. In the plots of Figure 10, the feasible aircraft are indicated in green and the non-feasible aircraft are indicated in red.

The planform of the initial aircraft and the optimized aircraft are shown in Figure 11. From this figure, several observations can be made. The sweep is increased considerably to 48 deg on the two outer most sections. This increase is mainly driven by the drag divergence Mach number and the longitudinal stability. It has some consequences that can be seen in Figure 11. The additional leading edge sweep causes a larger shift in center of gravity over the flight as well as during ground operations. The fuel is located in the outer two most sections, which lie further aft due to the higher sweep angle. The distance between the most forward and aft position of the center of gravity is increased. This means that the maximum and minimum load on the nose landing gear are closer to the limits of 5% and 20%, respectively.

The payload-range diagrams of the first and final aircraft are displayed in Figure 12. From the figure it can be observed that the harmonic range increases, as well as the ferry range. Another observation is the decrease in operating empty weight. During the optimization the MTOW is kept constant. The payload is constant as well, which means that when the OEW reduces, the fuel weight automatically increases in favor

^aOn an Intel Core 2 Duo T6400, 2.0 GHz CPU, with 4 GB RAM

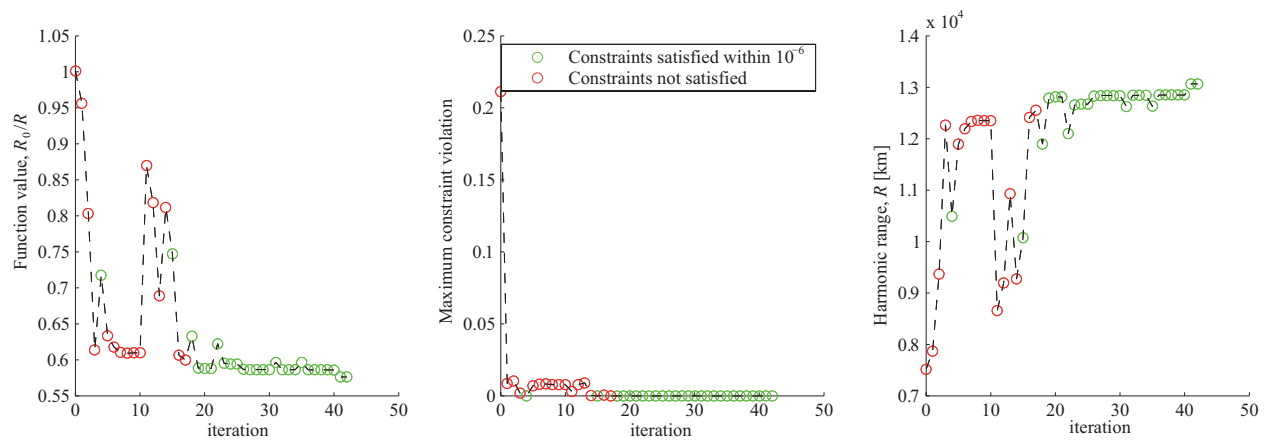


Figure 10. Function value, maximum constraint violation and maximum-payload range

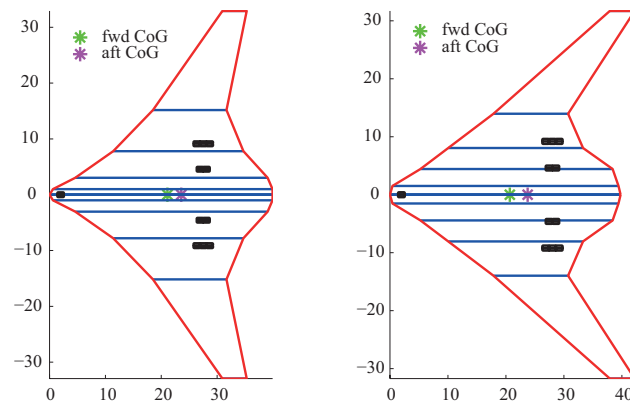


Figure 11. Initial aircraft (left) versus optimized aircraft (right)

of additional range. The second part of the payload-range diagram is smaller. This is the part where payload is exchanged for fuel to achieve additional range. The smaller second part of the payload-range diagram indicates that the fuel tanks are almost full for the harmonic range.

Figure 13 gives a summary of the most important parameters, the constraints and the objective. A blue number indicates that the constraint is satisfied. Since the aircraft is made feasible, all constraints are indicated in blue. The optimizer indicates in the MATLAB command window that there are no active boundaries and constraints. There are, however, some constraints that are very close to their limits, which have driven the optimization. One of these is the drag divergence Mach number of the second outer most section. This constraint has mainly driven the leading edge sweep and the thickness of the wing sections surrounding it. The minimum static margin is -9% MAC, close to the requirement of -10%, which has contributed to the larger sweep angle, moving the neutral point further aft.

The cabin floor area is not exactly at its limit, but is the main driver of the thickness of the center body. The reason that it is not exactly matching the requirement, is that the cabin floor area is not a perfectly smooth function. This is caused by the presence of the multi-bubble structure. The maximum-payload range increases to more than 13,000 km, which is higher than the initially assumed 11,000 km. The empty weight is slightly below the empty weight calculated during the preliminary sizing. The lift-to-drag ratio was assumed to be 23.4 during the preliminary sizing, but was predicted to be 24.2 in the aerodynamic analysis. Minimizing the trim drag is a possible way to increase the range, which can be observed during the optimization process as well. The maximum amount of elevator deflection required to balance the aircraft is limited to 4.7 deg whereas it was 5.7 deg at the start of the optimization, despite the fact that the center of

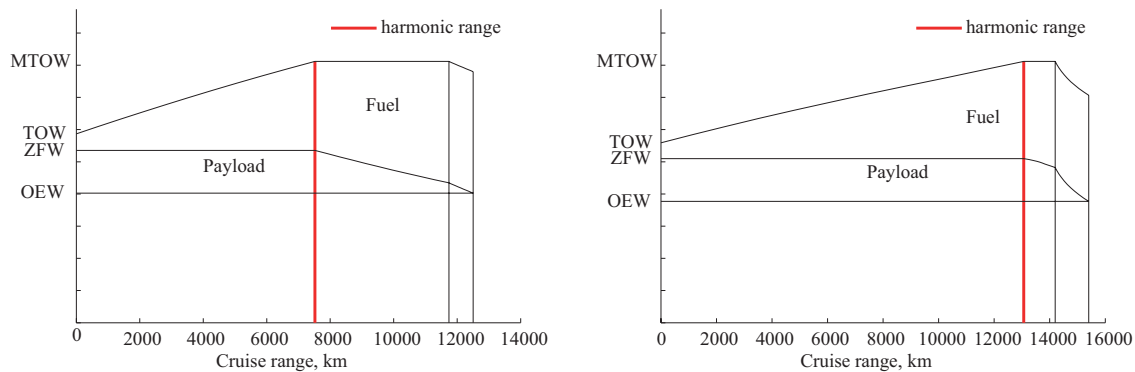


Figure 12. Initial aircraft (left) versus optimized aircraft (right) payload-range diagram

gravity travel during flight increased from 12% to 16% due to the increased sweep angle. The average fuel burn is 2.9L/pax/100km measured over the harmonic range of the aircraft. The aspect ratio lies close to the initial assumed value of 4 and the maximum lift coefficients are close to their initial estimates as well. A three-view of the optimized airplane can be seen in Figure 14.

IV. Conclusions and Future Work

A multi-disciplinary design and optimization framework for blended-wing-body aircraft has been developed. This tool is able of converting a given set of top-level requirements into a conceptual airplane design. It requires user input on configuration design variables such as vertical tail positioning, engine location, and forward-swept of aft-swept wing design. In the optimization process a set of 30 design variables are altered by a gradient-based optimizer. The design is subjected to 27 nonlinear and 4 linear constraints. Once feasible, the design is optimized for maximum harmonic range. It has been shown that this optimization requires between 20 and 60 iterations to converge, which takes up to 5 hours on a standard PC. For every constraint it is shown how close the optimized design approaches it, which gives feedback on the constraints that drive the design of the BWB. This tool is a first step in tackling the multi-disciplinary design problem of the BWB. The tool is to be improved in various areas. First of all, the analysis methods are to be refined by comparing the results to those of higher fidelity models. The output of the preliminary sizing module is to be improved by relying on the results of previously optimized BWB configurations. This should result in a better initial estimate for maximum take-off weight, wing loading and thrust-to-weight ratio and should contribute to a shorter number of iterations. Another measure to reduce the optimization time is by reducing the number of design variables without violating the number of designs that can be obtained. A new parametrization model for the center body is being developed that accomplishes that.

Acknowledgements

The authors would like to acknowledge Dr. E. Torenbeek for sharing his insights on non-conventional airplane configurations and introduction to relevant literature.

References

- ¹Schut, J. and van Tooren, M. J. L., "Design Feasibilization Using Knowledge-Based Engineering and Optimization Techniques," *Journal of Aircraft*, Vol. 44, No. 6, 2007, pp. 1776–1786.
- ²Wood, R. M. and Bauer, S. X. S., "Flying Wings / Flying Fuselages," *Proceedings of AIAA*, No. 2001-0311, Sept. 2001.
- ³Foa, J. V., "Suitability of Flying Wings as Jet Airplanes," *Journal of Aeronautical Sciences*, Vol. 16, No. 4, 1949, pp. 253–254.
- ⁴Torvik, P. J., "On the Maximum Range of Flying Wings," *Proceedings of AIAA*, No. 92-4223, August 1992.
- ⁵Torenbeek, E., "Aerodynamic Performance of Wing-Body Configurations and the Flying Wing," *presented at General, Corporate and Regional Aviation Meeting and Exposition*, ASME, Wichita, KS, April 1st 1991.

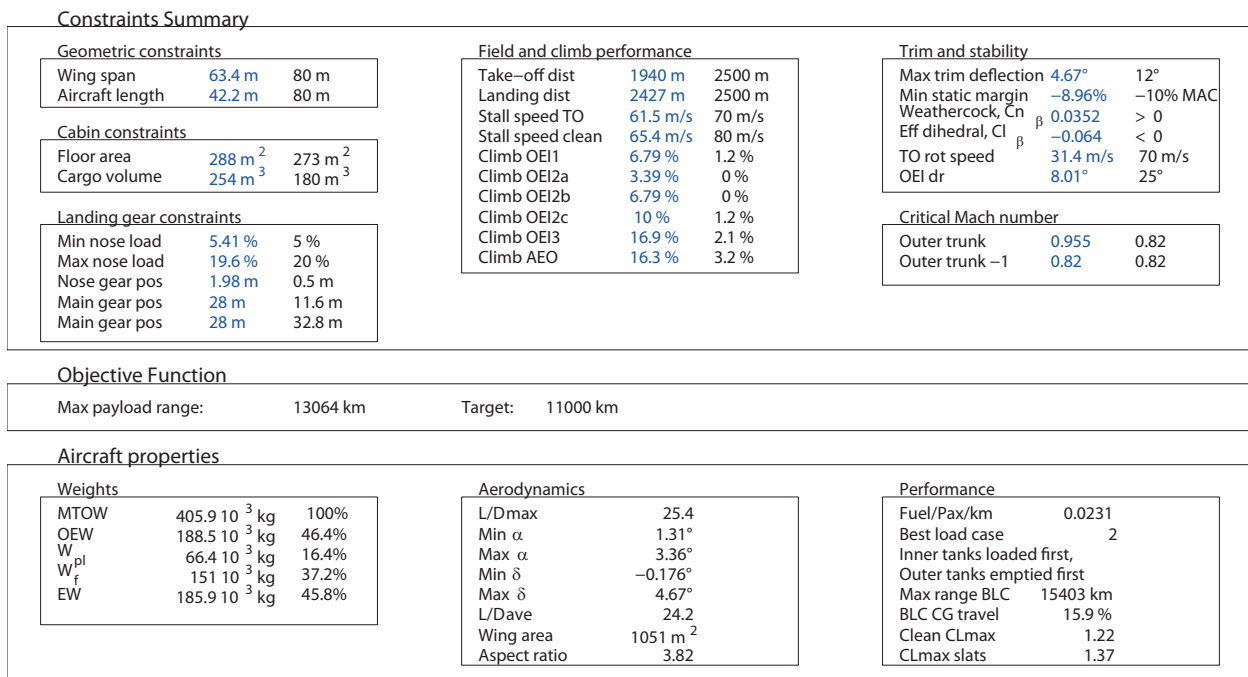


Figure 13. Summary displaying constraints, objective and other information

⁶Denisov, V. E., Bolsunovsky, A. L., Busoverya, N. P., and Gurevich, B. I., "Recent Investigations of the Very Large Passenger Blended-Wing-Body Aircraft," *Proceedings of the 21st Congress of International Council of the Aeronautical Sciences*, ICAS, Melbourne, Australia, 13-18 September 1998.

⁷Liebeck, R. H., Page, M. A., and Rawdon, B. K., "Blended wing body subsonic commercial transport," Tech. Rep. AIAA-98-0438, The Boeing Company Phantom Works, July 1998.

⁸Liebeck, R., "Design of the Blended Wing Body Subsonic Transport," *Journal of aircraft*, Vol. 41, 2004, pp. 10 – 25.

⁹Mecham, M., "New Tests Pending for X-48 Flying Wing," *Aviation Week*, September 2010.

¹⁰Wood, R. M., "The Contributions of Vincent Justus Burnelli," *Proceedings of AIAA*, No. 2003-0292, Jan. 2003.

¹¹Wakayama, S., "Blended-Wing-Body Optimization Problem Setup," *Proceedings of the 8th AIAA/USAF/NASA/ISSMO Symposium on Multidisciplinary Analysis and Optimization*, Long Beach, CA, 6-8 September 2000.

¹²Wilcox, K., "Design and Optimization of Complex Systems," .

¹³la Rocca, G., Krakkers, L., and van Tooren, M., "Development of an ICAD Generative Model for Blended Wing-Body Aircraft Design," *Proceedings of the 9th AIAA/ISSMO Symposium on Multidisciplinary Analysis and Optimization*, Atlanta, GA, 4-6 September 2002.

¹⁴la Rocca, G. and van Tooren, M. J. L., "Knowledge-based engineering approach to support aircraft multidisciplinary design and optimization," *Journal of Aircraft*, Vol. 6, 46, pp. 1875–1885.

¹⁵Straathof, M. and van Tooren, M., "Extension to the Class-Shape-Transformation Method Based on B-Splines," *AIAA Journal*, Vol. 49, No. 4, 2011, pp. 780–790.

¹⁶van der Laan, A. and van Tooren, M., "Parametric Modeling of Movable for Structural Analysis," *Journal of Aircraft*, Vol. 42, No. 6, 2005, pp. 1605–1613.

¹⁷Lisandrini, P. and van Tooren, M. J. L., "High-Order Finite Elements Reduced Models for Use in a Flutter Design Tool," *Journal of Aircraft*, Vol. 42, No. 3, 2005, pp. 748–754.

¹⁸Krakkers, L., van Tooren, M., and Schut, J., "A Design and Engineering Engine to Investigate Acoustics in Preliminary Fuselage Design," *Proceedings of the 9th AIAA/CEAS Aeroacoustics Conference and Exhibit*, Hilton Head, SC, May 12-14 2003.

¹⁹Baluch, H. and van Tooren, M., "Modified Inertially Coupled equations of motion for flexible aircraft with coupled vibrations," *Journal of Aircraft*, Vol. 46, No. 1, 2009, pp. 107–115.

²⁰Voskuil, M., la Rocca, G., and Dircken, F., "Controllability of blended wing body aircraft," *Proceedings of the 26th international congress of the aeronautical sciences*, edited by I. Grant, ICAS, Anchorage, AK, 14-19 September 2008.

²¹Österheld, C., Heinze, W., and Horst, P., "Preliminary Design of a Blended Wing Body Configuration using the Design Tool PrADO," *CEAS Conference on Aircraft Design and Optimization*, 25-26 June 2002.

²²Mukhopadhyay, V., Sobieszczanski-Sobieski, J., Kosaka, I., Quinn, G., and Charpentier, C., "Analysis Design and Optimization of Non-cylindrical Fuselage for Blended-Wing-Body (BWB) Vehicle," *Proceedings of the 9th AIAA/ISSMO Symposium on Multidisciplinary Analysis and Optimization*, Atlanta, GA, 4-6 September 2002.

²³Melin, T., "A Vortex Lattice MATLAB Implementation for Linear Aerodynamic Wing Applications," 2000.

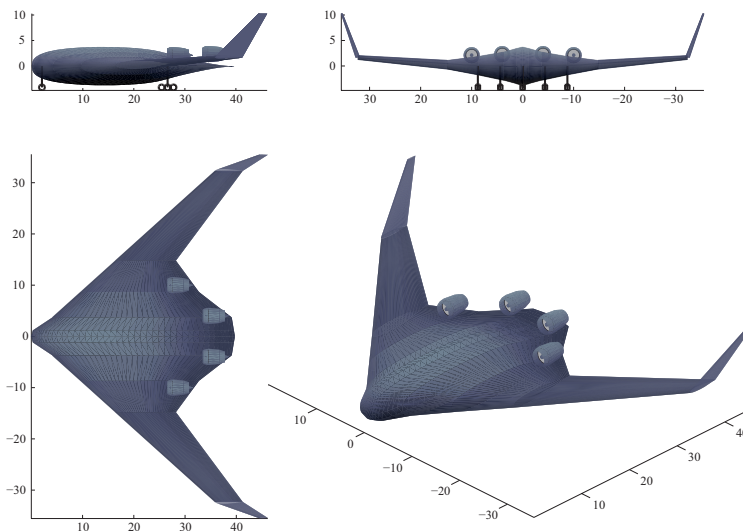


Figure 14. Three-View of Optimized BWB Configuration

²⁴Roskam, J., *Airplane Design Part V: Component Weight Estimation*, DARcorp, Lawrence, KS, 2003.

²⁵Raymer, D., *Aircraft design: A conceptual approach*, American Institute of Aeronautics and Astronautics, Washinton, DC, 2006.

²⁶Torenbeek, E., "Development and Application of a Comprehensive, Design-sensitive Weight Prediction Method for Wing Structures of Transport Category Aircraft," Tech. rep., Delft University of Technology, Department of Aerospace Engineering, 1992.

²⁷Geuskens, F., Koussios, S., Bergsma, O., and Beukers, A., "Non-Cylindrical pressure fuselages for future aircraft," *Proceedings of the 49th AIAA/ASME/ASCE/AHS/ASC Structures, Structural Dynamics, and Materials Conference*, No. 2008-1907, April 2008.

²⁸Anon., "Matlab R2011a Documentation, Optimization Toolbox, fmincon," Website, www.mathworks.com, accessed August 2011.